Int J Adv Manuf Technol (2009) 43:117–126
DOI 10.1007/s00170-008-1682-3

ORIGINAL ARTICLE

# Effect of delay time on part strength in selective laser sintering

**Prashant K. Jain · Pulak M. Pandey · P. V. M. Rao**

Received: 11 March 2008 / Accepted: 24 July 2008 / Published online: 12 August 2008
© Springer-Verlag London Limited 2008

**Abstract** Selective laser sintering (SLS) is one of the most popular layered manufacturing processes used for making functional prototypes of polymers and metals. It is a powder-based process in which layers of powder are spread and laser is used to sinter selected areas of preheated powder. In the present work, experimental investigations have been made to understand effect of delay time on SLS prototypes. Delay time is the time difference for laser exposure between any two adjacent points on successive scanning lines on a layer. Tensile specimens of polyamide material as per the ASTM standard are fabricated on SLS machine keeping delay time range constant for the entire specimen. Specimens are fabricated for different ranges of delay time and tested on universal testing machine for tensile strength. An optimum value of delay time range is obtained experimentally. As delay time depends on part build orientation, an algorithm has been developed and implemented to find out optimum part build orientation for improving tensile strength. The obtained results from developed code are validated experimentally for tensile specimen. Case study for a typical 3D part is also presented to demonstrate the capabilities of developed algorithm.

**Keywords** Selective laser sintering · Scan length · Delay time · Part strength · Part build orientation

P. K. Jain · P. M. Pandey (✉) · P. V. M. Rao
Mechanical Engineering Department,
Indian Institute of Technology Delhi,
New Delhi, India
e-mail: pmpandey@mech.iitd.ac.in

## 1 Introduction

Rapid prototyping (RP) is a generative manufacturing process which is used in engineering for producing conceptual models and functional prototypes. The application of RP has greatly shortened design manufacturing cycle time, hence facilitated in reducing cost of product and increasing competitiveness [1, 2]. RP is a material additive process in which computer-aided design model is tessellated and sliced in layers and product is produced by depositing one layer over other. The distinctive characteristic of this method is that geometric complexity of the part is unimportant. Commercial RP systems available today are stereolithography (SL), selective laser sintering (SLS), fused deposition modeling, laminated object manufacturing and three-dimensional printing, etc. [3, 4].

SLS is a powder-based RP technology that allows generating complex 3D parts layer by layer [5, 6]. Geometric model of the object is first tessellated and sliced into layers to get contour information of each layer. This layer contour information is used to sinter the selected areas of each layer while producing part [7]. SLS uses fine powder which is spread by a re-coater on the machine bed and scanned selectively using laser beam such that surface tension of grains is overcome and they are sintered together. Before the laser scans, entire machine bed is preheated to just below the melting point of material. Laser power is adjusted to bring selected powder areas to a temperature just sufficient for powder particles to get sintered. Build platform moves down by one layer thickness to facilitate new powder layer, and process is repeated for all subsequent layers to complete the part. Sintered material forms part, whilst un-sintered powder remains in its place to support the structure and may be cleaned away once the part is complete. SLS can be used to process any material,

provided it is available in the form of powder and that the powder particles tend to fuse or sinter when heat is applied [8]. Due to varied material capabilities, SLS process now stands as an alternative to conventional manufacturing techniques in certain applications like aerospace, automotive and biomedical applications. Because of the wide range of materials it can process, SLS is superior to other rapid manufacturing techniques. The powder materials which can be sintered include wax, cermets, ceramics, nylon/glass composites, metal-polymer powders, metals, alloys, steels and polymers [9].

Nowadays, RP is emerging as a rapid manufacturing technique which produces functional parts in small batches, particularly in aerospace application and rapid tooling. Therefore, prototypes should have sufficient strength to ensure proper functional requirements. However, parts produced by SLS show lower strength and shorter functional life than the parts produced by conventional polymer processing techniques such as injection moulding [10, 11]. Several attempts have been made to study effect of process parameters on mechanical properties of SLS prototypes. Gibson and Shi [12] investigated effect of laser power, hatch spacing and scan size on strength and density of RP parts using fine nylon material. Thompson and Crawford [13] examined effect of process parameters, namely, laser power, layer thickness and build orientation, on surface roughness and tensile strength and developed regression models. Williams and Deckard [14] used analytical and experimental methods to study effect of energy density, spot diameter and delay on average density and strength of bisphenol polycarbonate parts. It was found that for a given set of parameters, namely, laser power, beam speed and hatch spacing, there exists an optimum delay range in which parts have maximum density and strength in terms of flexural modulus. Yang et al. [15] used space filling fractal curves for generating scanning pattern. They compared fractal pattern with conventional linear pattern experimentally. They reported that fractal path scanning yields improved physical properties. They compared temperature field generated by two patterns and found that temperature field of fractal path is smoother than the conventional one.

Ning et al. [16] investigated effect of hatch length variation on material anisotropy and heterogeneity of parts built by direct metal laser sintering process. They concluded that very short hatch lines make part more heterogeneous than the larger ones. Since hatch line length varies with hatch direction, they developed code for determining optimum hatch direction for each layer of parts using genetic algorithm. It was found that orientation and hatch direction affect anisotropy as well as part strength. Hatch line lengths also affect part strength, and the same is found to be higher for short hatch lines as compared to long hatch lines. Caulfield et al. [17] studied influence of energy density (which is a combination of laser power, beam speed and hatch spacing) in SLS process on the mechanical properties of polyamide components and found that parts fabricated at high energy density levels show more ductile behaviour than the parts fabricated at low energy density levels. It was also reported that Young's modulus, yield strength and fracture strength increases with an increase in energy density. Recently, Jain et al. [18] conducted experimental study to investigate effect of delay time on tensile strength of SLS parts while keeping primary process parameters such as laser power, laser beam speed, hatch spacing and part bed temperature constant. It was found that secondary process parameter, i.e. delay time, has significant influence on part strength. They developed a novel method to vary delay time range for fabrication of tensile specimen in different delay time ranges.

Literature review presented above reveals that the effect of parameters such as laser power, beam speed and hatch spacing which together define energy density has been investigated in detail. It was felt that delay time has not been paid much attention. Delay time is a time difference between any two adjacent points on successive scanning lines (Fig. 1) and depends on laser beam speed and layer geometry [14] which can be varied by changing part build

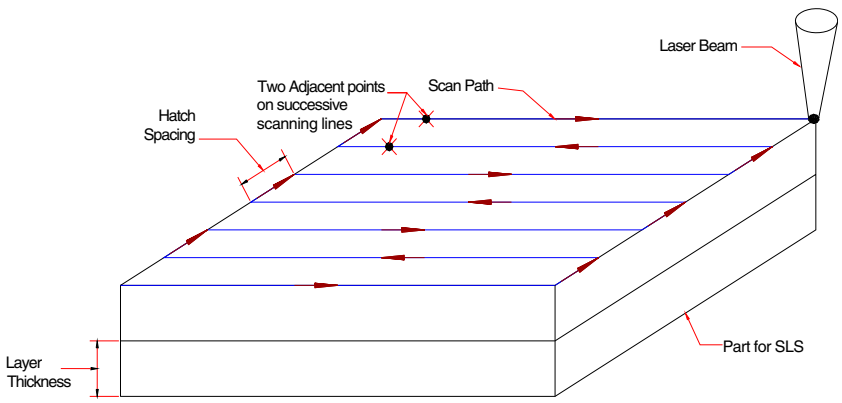


**Fig. 1** Laser sintering schematics

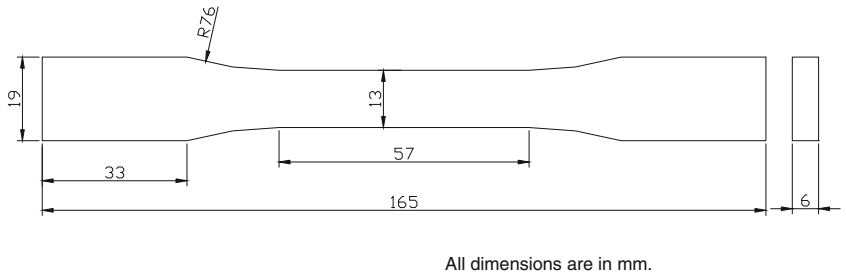


**Fig. 2** Dimensions of the tensile test specimen as per ASTM D638

orientation. Some studies reported orientation effects on the part strength without considering delay time effect [12, 14, 16, 17], but no effort has been made to study the orientation effect on part strength by considering delay time. Authors have already reported significant effect of delay time on part strength in their previous attempt [18].

In the present work, an attempt has been made to study the effect of delay time on strength of SLS parts using polyamide powder and to find optimum part build orientation. Tensile test specimens are fabricated in various delay time ranges. Fabricated specimens are tested for ultimate tensile strength on universal testing machine. Optimum value of delay time range is obtained experimentally. An algorithm has been developed and implemented in MATLAB to find out optimum part build orientation for improved tensile strength. The obtained results from developed code are experimentally validated. Part deposition orientation of a typical 3D part is also presented to demonstrate the capabilities of developed algorithm. The contribution of this paper is to study coupling between part orientation and delay time and use the results to find out optimum part build orientation for better part strength in SLS process.

## 2 Details of experiments

In order to study the mechanical strength of SLS parts, tensile test specimens are fabricated as per ASTM D638 standard (Fig. 2) on a commercial EOSINT P380 workstation. Material used in this study is polyamide (PA 2200) of average grain size 60 μm supplied by M/s Electro Optical Systems (EOS), Germany. Fabricated specimens are tested for ultimate tensile strength on universal testing machine. An optimum value of delay range has also been obtained experimentally. The details of the experimental procedure followed have been presented below.

### 2.1 Fabrication of tensile test specimens

Since SLS machine does not have provision to fabricate parts with different delay time ranges, a scheme for fabrication has been designed so that tensile specimens can be produced for a constant delay time. Corresponding STL files are imported in to Magics® software, and the specimens are laid down along with strips on the build platform as shown in Fig. 3. Each tensile specimen is fabricated along with two rectangular strips; each one is on either side of the specimen. As delay time between two successive exposures is directly proportional to scan length for a constant scan speed, by adjusting distance between rectangular strips, required delay time range for each specimen is obtained. Figure 3 shows one such arrangement to achieve delay range of 0.014–0.021 s. Here, unsorted scanning option available on the SLS machine control software has been used for laser scanning of layer geometry so that laser has to move from left strip to right strip with the same velocity, i.e. scan velocity, irrespective of whether laser is switched on or off. Skywriting option is used so that acceleration and deceleration of laser beam is kept outside the layer geometry. The times involved in acceleration and deceleration is very small and neglected in

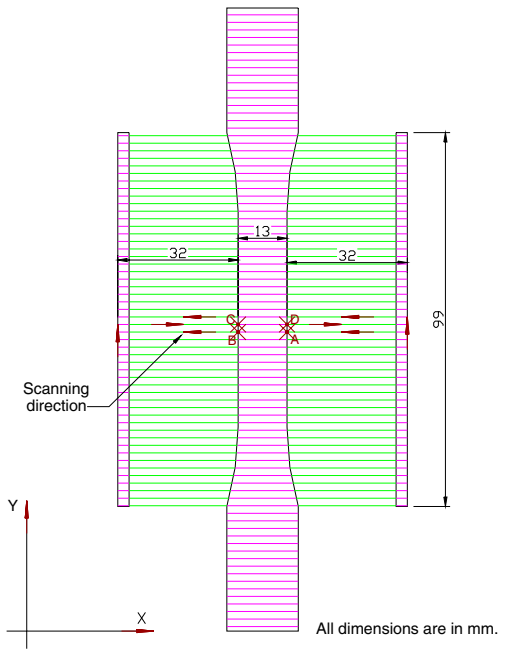


**Fig. 3** Special design of specimen for varying delay time range (0.014–0.021 s)

delay time calculation. Delay time ($T_d$) can be calculated as follows:

$$T_d = \frac{D}{V} \quad (1)$$

where $D$ is distance travelled by laser beam to scan two consecutive points in millimetre and $V$ is laser beam speed in millimetre per second. $D$ is twice the distance of points from rectangular strip in scanning direction. For example, points A and D and points B and C are the points where two successive exposures of laser occur (Fig. 3). At point 'C', delay is $\frac{32\times2}{4500} = 0.01422$ s and at point 'D' $\frac{(32+13)\times2}{4500} = 0.02$ s at scan speed 4,500 mm/s. This shows that all the points on gauge length area of tensile specimen fall within delay range of 0.014–0.021 s. Distance of rectangular strips for all the specimens has been taken in such a way that all the points on the gauge length area fall within the required delay range. For fabrication planning, STL files of tensile specimens along with strips are arranged in Magic's software.

All experiments were repeated thrice for repeatability for seven different delay time ranges, ranging from 0–0.049 s in the increments of 0.007 s. To avoid the effect of part temperature variation along the build platform, care has been taken and parts are fabricated at the same position on the build platform, i.e. at the centre of build platform. Values of process parameters like laser power, beam speed and hatch spacing are chosen based on manufacturer's manual and are given in Table 1. These values are also checked for maximum and minimum energy density because at higher energy density, material degrades and at lower energy density particle may not get sintered. Values of laser power, beam speed and hatch spacing together define energy density as given below [12, 14]:

$$E = \frac{P}{V \times H_s}. \quad (2)$$

Here, $E$ is energy density in joules per square millimetre, $P$ is laser power in watts, $V$ is laser beam speed in millimeter per second and $H_s$ is hatch spacing in millimetre. It is reported in previous works [19, 20] that sintering does not occur if value of $E$ is below 1 J/cm$^2$ and polymer degradation starts above 4.8 J/cm$^2$ in case of polyamide material. Hence, suitable energy density used in the present work is, i.e. 2.74 J/cm$^2$. Phenomenon of curling is observed when part bed temperature is less than 175°C, and if it is beyond 178°C, caking occurs. Curling is a phenomenon in which sintered layers become non-planer due to high thermal gradient between sintered and un-sintered powder material. Caking is a phenomenon in which powder particles stick together and large amount of powder forms as lump and moves with re-coater. Scan pattern is selected along X-direction and kept the same for all layers of the tensile specimen.

**Table 1** Process parameters used in experimentation

| Laser power | Beam speed | Hatch spacing | Part bed temperature |
|---|---|---|---|
| 37 W | 4,500 mm/s | 0.3 mm | 175°C |

### 2.2 Tensile testing of specimens

A total of 21 specimens, three for each delay range under investigation, are fabricated and tested for ultimate tensile strength. The crosshead speed during tensile test was kept at 5 mm/min, and data were recorded at a rate of ten points per second. The obtained values of average ultimate tensile strengths of the specimens corresponding to their delay time range are presented in Fig. 4. It can be seen from Fig. 4 that there exists a delay time range for polyamide material which gives maximum tensile strength for a given set of SLS process parameters, namely, laser power, scan speed, hatch spacing, scan direction and part bed temperature. From Fig. 4, it is evident that 0.007–0.014 s is the optimum delay time range for polyamide.

## 3 Part strength improvement

The time difference between successive exposures (delay time) at a point on the part layer is controlled by the length of scan line and speed of laser beam. The length of scan line depends upon the orientation of part. Improper orientation may lead to either very small or very large delay time between successive exposures, which results into improper binding between powder particles. Scan length and delay period influence strength of prototypes significantly. Experiments conducted in this work have shown that a part can have improved strength at an

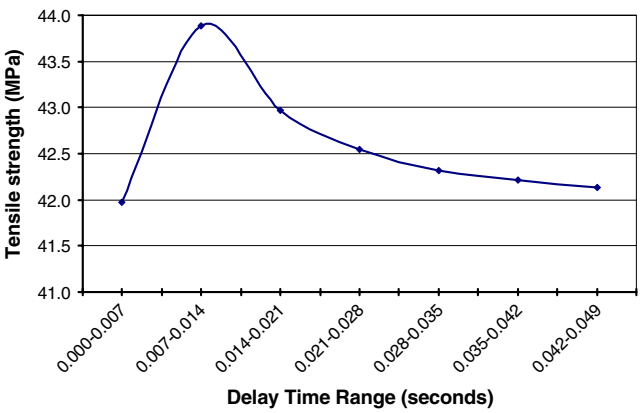


**Fig. 4** Tensile strength vs delay time range

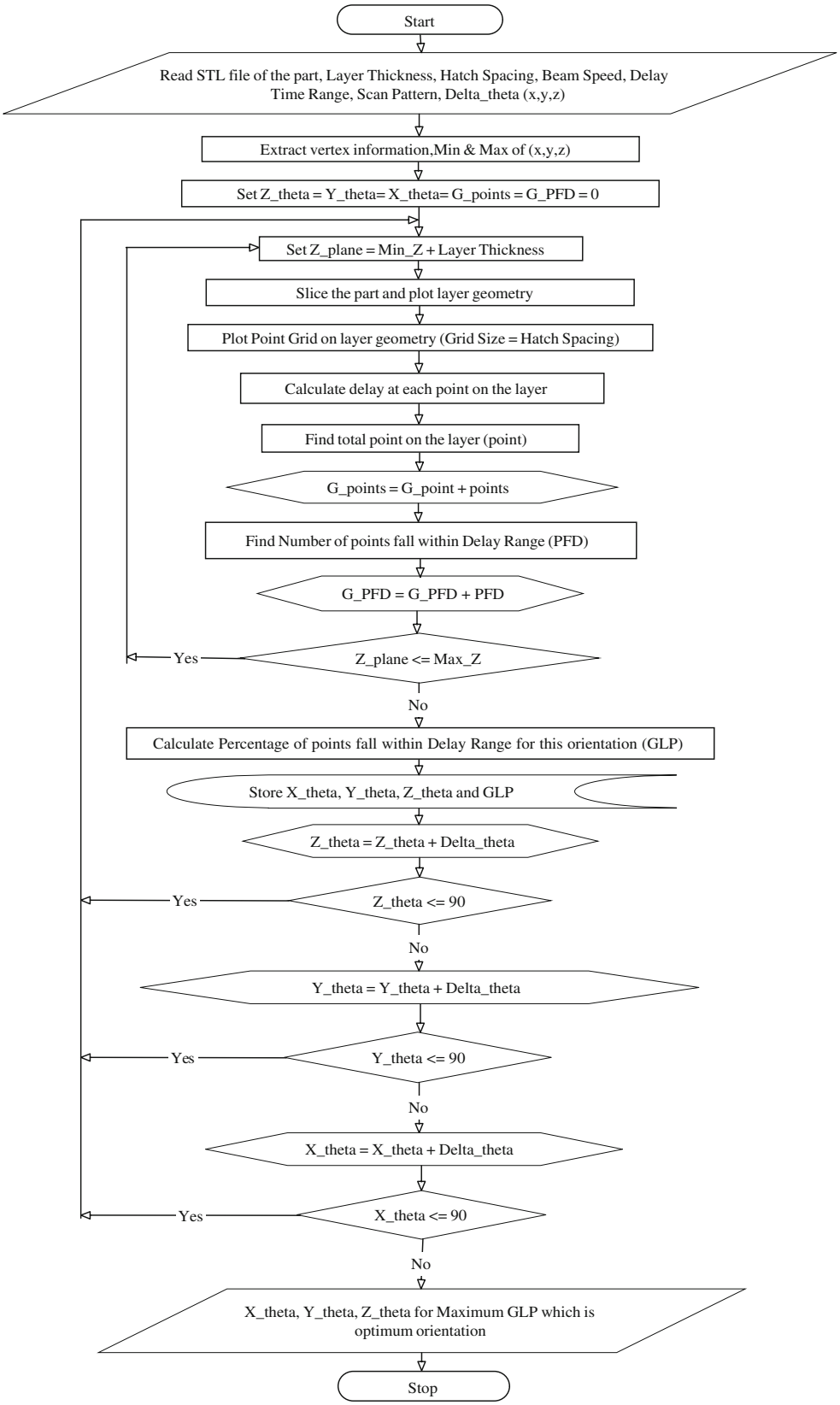


**Fig. 5** Flow chart for implementation procedure

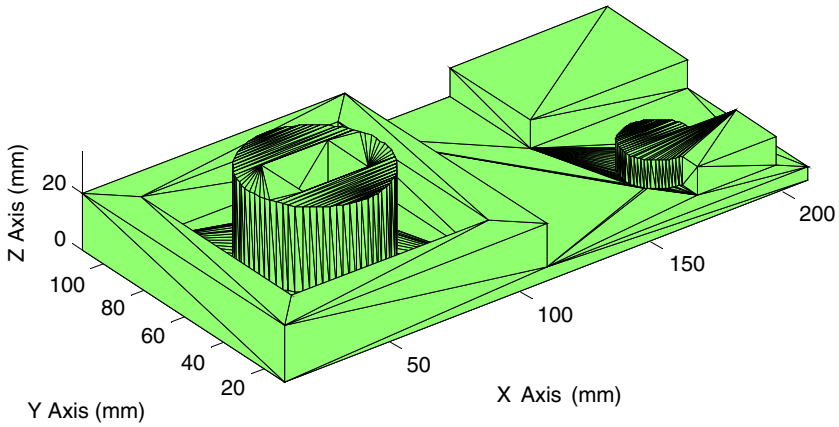


**Fig. 6** STL file of a typical 3D part (considered for case study) imported in MATLAB

orientation in which maximum area of all layers to be sintered falls within the optimum delay time range.

An algorithm is therefore developed to find build orientation of a part in which maximum area on all layers of the part falls within the optimum delay time range and supposed that this orientation will give maximum strength. In this algorithm, STL file of part is orientated at various orientations on build platform; for every orientation, corresponding STL file is sliced and geometry of each layer plotted along with a grid of spacing equal to hatch spacing. Delay time at all grid points on layer geometry is calculated. Those points for which delay time fall within the optimum delay range are counted. Total number of grid points is also counted on layer geometry. This process is repeated for all layers. Percentage of points (GLP) for which delay time falls within optimum delay range on all layers at a particular orientation is calculated as given below.

$$GLP = \frac{\sum_{i=1}^{n} PFD_i}{\sum_{i=1}^{n} P_i} \times 100 \quad (3)$$

where $PFD_i$ is number of points for which delay time falls within optimum delay range for $i$th layer, $P_i$ is number of grid points that fall within the part geometry on $i$th layer and $n$ is number of layers. Obtained GLP is considered as a criterion to maximise part strength. Part build orientation which gives maximum GLP is supposed to give maximum part strength. A flow chart showing implementation procedure for above discussed algorithm is presented in Fig. 5.

To implement the developed algorithm in MATLAB-7, STL file of the part is used as input to MATLAB program as shown in Fig. 6. Various parameters like hatch spacing, scan speed, layer thickness, optimum delay range and scanning direction/pattern are also taken as inputs to the program. To find contour of the geometry at a particular height, a plane at that height is considered, and all triangles intersecting with this plane are found and their intersection points with this plane calculated as shown in Fig. 7. These points are stored in sequence as found in the STL file than checked for multiple contours and arranged accordingly. Obtained contours are separated as internal and external contours to find desired area for laser scanning as shown in Fig. 8. Finally, sintering area has been calculated for a particular layer by generating a grid (rectangular array at known point spacing) of points, and number of grid points which fall within the part geometry is counted ($P_i$). This

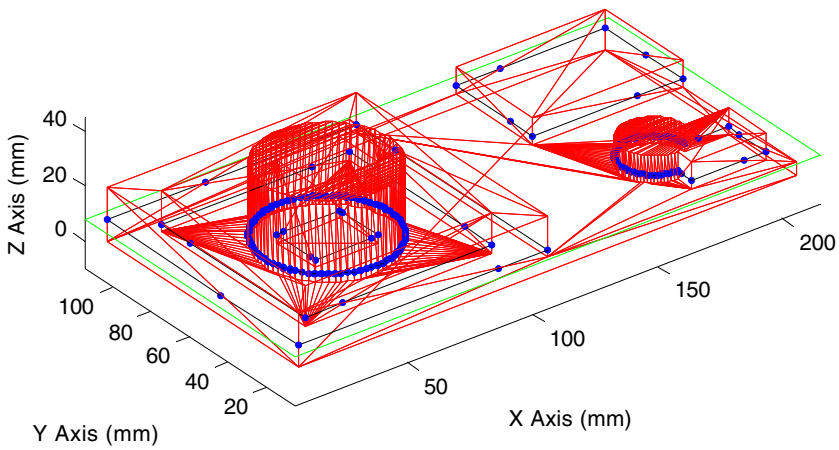


**Fig. 7** Intersection points calculated at particular height

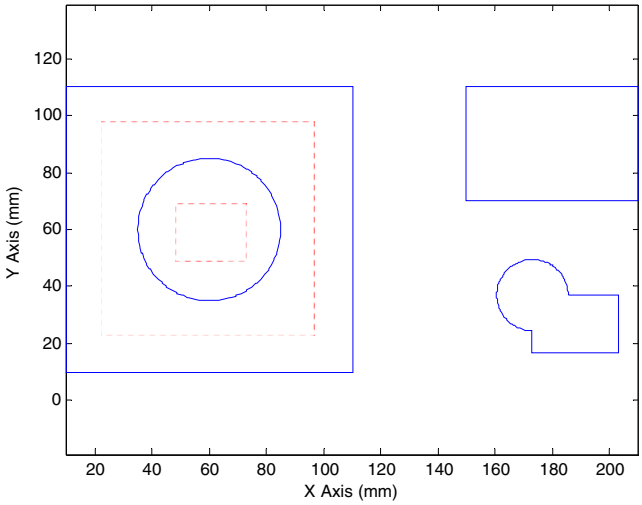


**Fig. 8** Multiple contours plotted as internal (*dashed line*) and external (*solid line*) contours

represents index of area to be sintered of corresponding layer geometry (Fig. 9). For all these points, delay time is also calculated, and the number of points for which delay time falls within the optimum delay range is counted ($PFD_i$). This represents the area that falls within the optimum delay range (Fig. 10).

The procedure is repeated for all possible part build orientations by rotating STL file about three axes, viz. *X*, *Y* and *Z*, with suitable angle interval. Program can be executed for any small angle, but it may be time-consuming. GLP is then calculated for all orientations, and maximum GLP is considered as the basis for selecting optimum part build orientation.

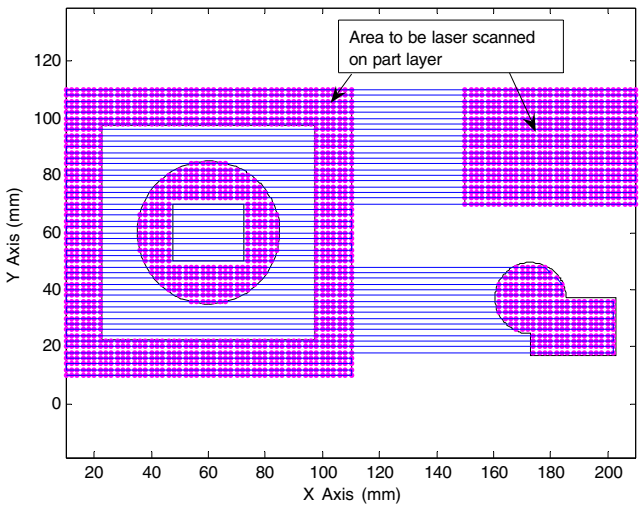


**Fig. 9** Grid points plotted on the part layer geometry along the scan path

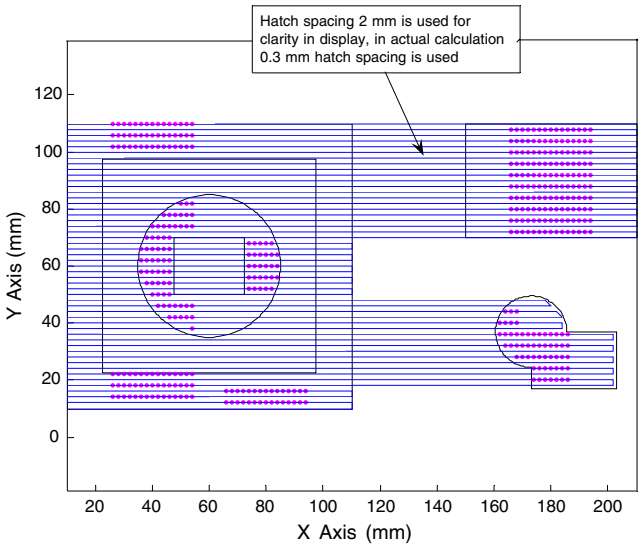


**Fig. 10** Grid points which fall within the optimum delay range on the part layer

## 4 Validation of algorithm

To validate the algorithm presented in the previous section, optimum build orientation of a tensile specimen is obtained and verified experimentally. GLP for tensile specimen is calculated through developed MATLAB program for all orientations in the range of 0–90° at an interval of 15° (Table 2). Here, layer thickness of 0.15 mm, hatch spacing of 0.3 mm and scan speed of 4,500 mm/s are considered for calculating values of GLP. It is evident from Table 2 that tensile specimen has maximum GLP at 60° orientation.

To verify the results obtained by the developed algorithm, tensile specimens are fabricated at different part build orientations in the range of 0–90° at an interval of 15°. All specimens are fabricated at centre of platform as shown in Fig. 11. The obtained values of ultimate tensile strengths of specimens corresponding to their orientations have been plotted in Fig. 12. It can be seen from Fig. 12 that maximum strength is observed at 60° orientation, and

**Table 2** Calculated *GLP* of tensile specimen at various orientations

| S. No. | Orientation (°) | GLP (%) |
|---|---|---|
| A1 | 00 | 8.73 |
| A2 | 15 | 9.92 |
| A3 | 30 | 13.95 |
| A4 | 45 | 26.44 |
| A5 | 60 | 40.71[a] |
| A6 | 75 | 29.28 |
| A7 | 90 | 11.23 |

[a] Orientation for maximum strength

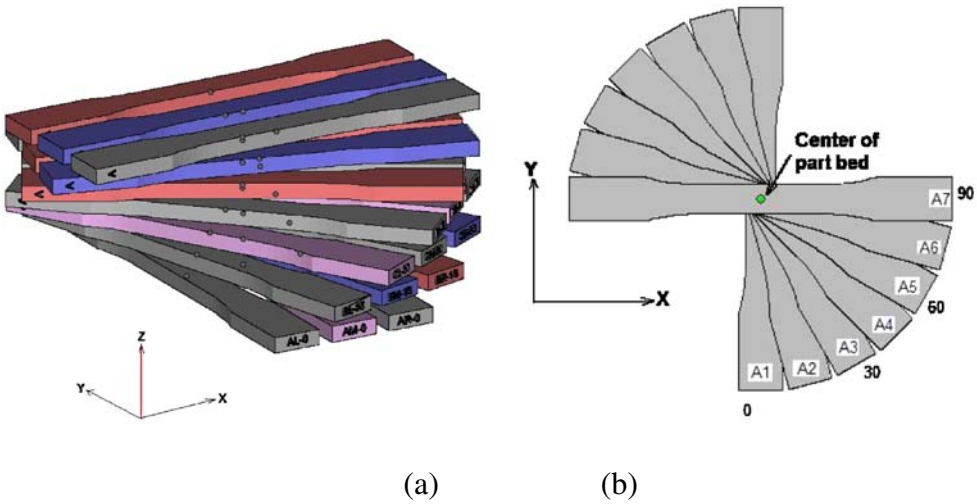


**Fig. 11** Arrangement of specimens on build platform for confirmation test for scanning direction along *X*-axis: **a** 3D, **b** top view

same is the prediction of the developed algorithm as presented in Table 2. Therefore, it is concluded that the developed algorithm in this work is able to predict the orientation which gives maximum strength for given values of process parameters based on delay time. It can be seen from Table 2 and Fig. 12 that the values of GLP for specimen A4 is marginally lower as compared to GLP of specimen A6, but the strength of A4 is marginally higher as compared to specimen A6. This algorithm is able to predict orientation of maximum strength and does not imply that strength is proportional to GLP.

A part with various geometric shapes having multiple contours is considered (Fig. 6) to demonstrate the capabilities of developed algorithm. Parameters considered are layer thickness of 0.15 mm, hatch spacing of 0.3 mm and scan speed of 4,500 mm/s for plotting grid on each layer and calculating delay time on each point. GLP is calculated for all orientations at an angle interval of 1°. Orientation for which calculated GLP found maximum is considered as optimum part build orientation. In Table 3, a sample output for 45° angle increment is given; however, the program can be executed for any small increment. Here, optimum part build orientation is found when $X_{theta}$=90°, $Y_{theta}$=45° and $Z_{theta}$=90° where $X_{theta}$, $Y_{theta}$ and $Z_{theta}$ are the angles of rotation about *X*-axis, *Y*-axis and *Z*-axis, respectively, in sequence and is shown in Fig. 13.

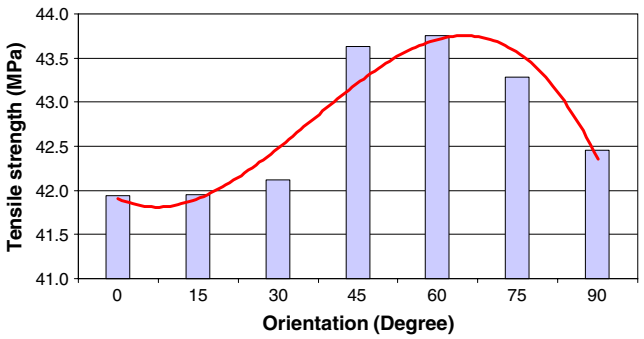


**Fig. 12** Graph showing tensile strength at various orientations obtained in confirmation test

**Table 3** Calculated GLP at various orientations with rotation about three axes for case study part

| S. No. | $X_{theta}$ | $Y_{theta}$ | $Z_{theta}$ | GLP |
|---|---|---|---|---|
| 1 | 0 | 0 | 0 | 24.94 |
| 2 | 0 | 0 | 45 | 29.13 |
| 3 | 0 | 0 | 90 | 28.96 |
| 4 | 0 | 45 | 0 | 64.21 |
| 5 | 0 | 45 | 45 | 60.68 |
| 6 | 0 | 45 | 90 | 42.67 |
| 7 | 0 | 90 | 0 | 69.40 |
| 8 | 0 | 90 | 45 | 61.49 |
| 9 | 0 | 90 | 90 | 47.66 |
| 10 | 45 | 0 | 0 | 40.84 |
| 11 | 45 | 0 | 45 | 59.30 |
| 12 | 45 | 0 | 90 | 68.26 |
| 13 | 45 | 45 | 0 | 59.29 |
| 14 | 45 | 45 | 45 | 68.26 |
| 15 | 45 | 45 | 90 | 65.85 |
| 16 | 45 | 90 | 0 | 62.60 |
| 17 | 45 | 90 | 45 | 69.40 |
| 18 | 45 | 90 | 90 | 63.73 |
| 19 | 90 | 0 | 0 | 43.82 |
| 20 | 90 | 0 | 45 | 59.89 |
| 21 | 90 | 0 | 90 | 68.87 |
| 22 | 90 | 45 | 0 | 49.83 |
| 23 | 90 | 45 | 45 | 63.95 |
| 24 | 90 | 45 | 90 | 69.86[a] |
| 25 | 90 | 90 | 0 | 48.68 |
| 26 | 90 | 90 | 45 | 60.95 |
| 27 | 90 | 90 | 90 | 69.40 |

[a] Orientation for maximum part strength

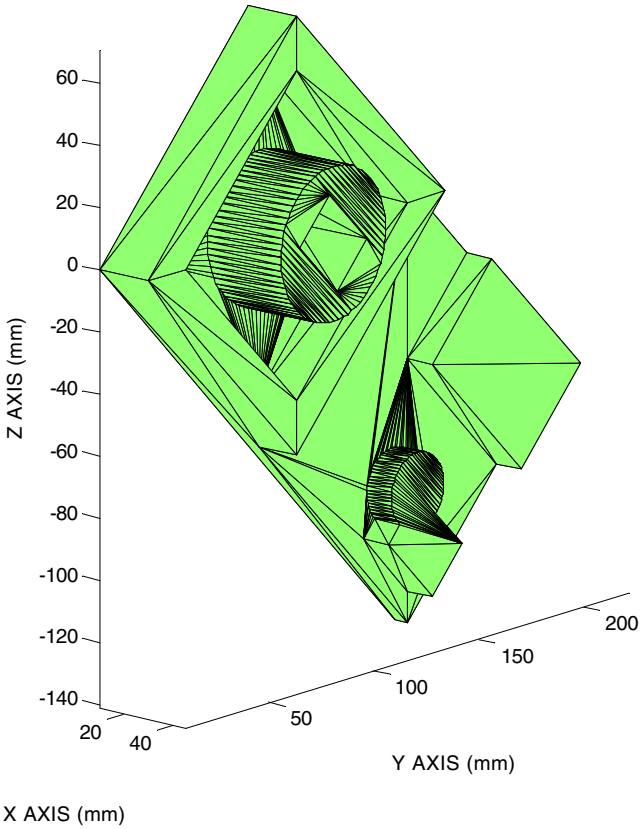


**Fig. 13** Obtained optimum part build orientation from the developed code

## 5 Discussions

The delay time between two adjacent points on successive scan lines depends on the length of scan line and speed of laser beam. The length of scan line can be varied by changing the orientation of the part. Parts may have either very small or very large delay time between successive exposures, which result into improper sintering characteristics. In some cases, very small or very large delay time can be avoided by proper orientation of the part. In this experimental work, it has been found that delay time influences the strength of prototypes significantly. Part strength increases with an increase in delay time range. Further increase in delay time range causes part strength to reach maximum value and then decrease. At low delay time range part strength is less and can be attributed to thermal degradation of polyamide powder. Further drop in the part strength is observed at higher delay time range, which happens due to insufficient bonding of polyamide powder particles. It can be seen from Fig. 12 that the strength in the range 0–30° orientation is lower as compared to 45–75°, and again, strength decreases when orientation is increased to 90°. This may be due to the reason that at 0–30° orientation, scan lines are very short (13–15 mm) and delay time ranges from 0 to 0.006 s; however, at 45–75° orientation, scan lines are medium (15–50 mm) in length and delay time ranges from 0 to 0.022 s. Above 75° orientation, scan lengths are very high (50–165 mm) and delay time ranges from 0 to 0.073 s. Optimum delay range happens somewhere in the middle around orientation angle of 60°. Proposed algorithm also predicts optimum orientation around 60° as presented earlier.

In this experimental study, loading direction and scanning direction are perpendicular to each other at 0° orientation, and it is parallel when at 90° orientation, as shown in Fig. 14. Strength is higher at 90° orientation as compared to 0° orientation. This may be due to the reason that delay time range is much wider (0–0.073 s), which includes optimum delay time range at 90° orientation as compared to 0° orientation where no area falls within optimum delay time range. It is obvious and it is also reported in literature [12, 16, 17, 21] that strength is likely to be more when scanning and loading directions are the same. This can also be attributed to anisotropy present in the material because of laser scanning direction; however, from the present study, it is concluded that it is not only the scanning direction but also the delay time values that affect the strength significantly. Ning et al. [16] also reported that orientation has significant influence on the part strength and the length of the hatch line affects it. The strength of built part using short scan lines is higher than that using long scan lines. But they have not studied effect of delay time which depends on scan length. In the present work, it has been found that strength is lower at shorter scan lengths as well as when scan lengths are longer.

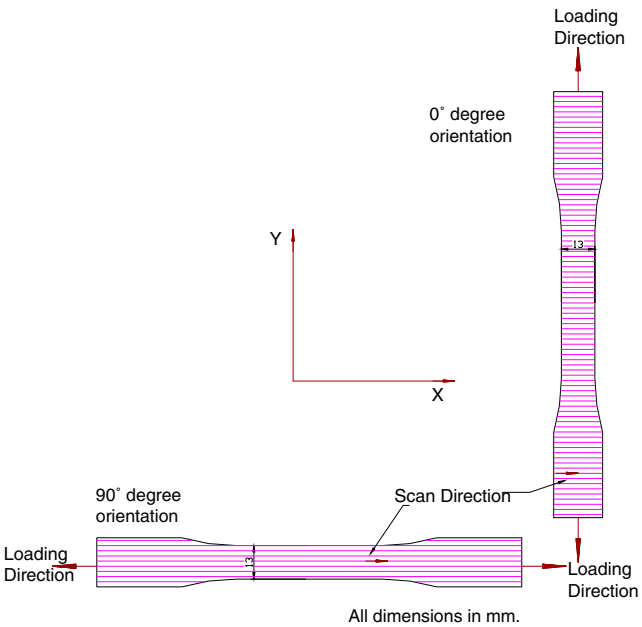


**Fig. 14** Tensile specimens showing scanning direction and loading direction

Part build orientation has been obtained for a typical 3D part (Fig. 6) and presented to demonstrate the capabilities of developed algorithm (Fig. 13). From the obtained result, it appears that the obtained part build orientation may effect surface finish and build time adversely. To avoid this situation, a multi-objective criteria decision making can be used with priority levels for better prototype quality. An alternative approach may be to first determine an orientation which gives minimum build height. Then, STL file of the modelled part should be rotated about the *Z*-axis, i.e. in *XY* plane only, to find optimum part build orientation which further improves part strength based on delay time.

## 6 Conclusions

In the present work, an attempt has been made to study the effect of delay time on tensile strength of SLS parts fabricated using polyamide powder. An optimum delay time range has been found experimentally. An algorithm has been developed and implemented successfully to predict part build orientation for improved part strength by considering delay time. The developed algorithm has been experimentally validated. It is concluded that comparatively higher strength can be achieved by orienting part so that maximum area on all layers falls within the optimum delay time range.

## References


1. Pham DT, Dimov SS (2001) Rapid manufacturing: the technologies and applications of rapid prototyping and rapid tooling. Springer, London
2. Tang Y, Loh HT, Fuh JYH, Wong YS, Lee HS (2005) An algorithm for disintegrating large and complex rapid prototyping objects in a CAD environment. Int J Adv Manuf Technol 25:895–901 doi:10.1007/s00170-003-1913-6
3. Chen YH, Ng CT, Wang YZ (1999) Generation of an STL File from 3D measurement data with user-controlled data reduction. Int J Adv Manuf Technol 15:127–131 doi:10.1007/s001700050049
4. Wang RJ, Wang L, Zhao L, Liu Z (2007) Influence of process parameters on part shrinkage in SLS. Int J Adv Manuf Technol 33:498–504 doi:10.1007/s00170-006-0490-x
5. Chua CK, Leong KF, Lim CS (2003) Rapid prototyping: principles and applications, 2nd edn. World Scientific, Singapore
6. Venuvinod PK, Ma W (2004) Rapid prototyping: laser based and other technologies. Kluwer, Boston
7. Pandey PM, Reddy NV, Dhande SG (2003) Slicing procedures in layered manufacturing: a review. Rapid Prototyping J 9(5):274–288 doi:10.1108/13552540310502185
8. Kruth JP, Wang X, Laoui T, Froyen L (2003) Lasers and materials in selective laser sintering. Assembly Autom 23(4):357–371 doi:10.1108/01445150310698652
9. Jain PK, Senthilkumaran K, Pandey PM, Rao PVM (2006) Advances in materials for powder based rapid prototyping. Proceedings of International Conference on Recent Advances in Materials and Processing. PSG College of Technology, Coimbatore, India, December 15–16
10. Pham DT, Dimov SS, Lacan F (1999) Selective laser sintering: applications and technological capabilities. J Eng Manuf 213: 435–449
11. Wang XC, Laoui T, Bonse J, Kruth JP, Lauwers B, Froyen L (2002) Direct selective laser sintering of hard metal powders: experimental study and simulation. Int J Adv Manuf Technol 19:351–357 doi:10.1007/s001700200024
12. Gibson I, Shi D (1997) Material properties and fabrication parameters in selective laser sintering process. Rapid Prototyping J 3(4):129–136 doi:10.1108/13552549710191836
13. Thompson DC, Crawford RH (1997) Computational quality measures for evaluation of part orientation in free form fabrication. J Manuf Syst 16(4):273–289
14. Williams JD, Deckard CR (1998) Advances in modelling the effects of selected parameters on the SLS process. Rapid Prototyping J 4(2):90–100 doi:10.1108/13552549810210257
15. Yang J, Bin H, Zhang X, Liu Z (2003) Fractal scanning path generation and control system for selective laser sintering. Int J Mach Tool Des Res 43:293–300
16. Ning Y, Wong YS, Fuh JYH (2005) Effect and control of hatch length on material properties in the direct metal laser sintering process. J Eng Manuf 219:15–25
17. Caulfield B, McHugh PE, Lohfeld S (2007) Dependence of mechanical properties of polyamide components on build parameters in the SLS process. J Mater Process Technol 182:477–488 doi:10.1016/j.jmatprotec.2006.09.007
18. Jain PK, Pandey PM, Rao PVM (2007) Experimental investigations into the effect of delay time on part strength in selective laser sintering. Proceedings of International Conference on Manufacturing Automation. National University of Singapore, Singapore, May 28–30, pp 501–516
19. Raghunath N, Pandey PM (2006) Improving accuracy through shrinkage modelling by using Taguchi method in selective laser sintering. Int J Mach Tools Manuf 47:985–995 doi:10.1016/j.ijmachtools.2006.07.001
20. Bacchewar PB, Singhal SK, Pandey PM (2007) Statistical modelling and optimization of surface roughness in selective laser sintering process. J Eng Manuf B 221:35–52
21. Ajoku U, Saleh N, Hopkinson N, Hague R, Erasenthiran P (2006) Investigating mechanical anisotropy and end-of-vector effect in laser-sintered nylon parts. J Eng Manuf B 220:1077–1086